UMYU Scientifica, Vol. 4 NO. 4, December 2025, Pp 338 – 358
https://doi.org/10.56919/usci.2544.030
ISSN: 2955 – 1145 (print); 2955 – 1153 (online)
A periodical of the Faculty of Natural and Applied Sciences, UMYU, Katsina

ORIGINAL RESEARCH ARTICLE

Development of Starch-based Biodegradable Plastics reinforced with Natural Fiber for enhanced mechanical and biodegradation properties

Dini Sabo[1], Shehu Habibu[1]*, Magaji Ladan[1], Shuaibu Abdullahi[2] and Daniel Eric[3]
[1]Department of Pure and Industrial Chemistry, Bayero University Kano, PMB 3011, Kano, Nigeria
[2]Department of Chemistry, Modibo Adama University, Yola, Nigeria
[3]Department of Chemistry, Nasarawa State University, Keffi, Nasarawa, Nigeria

ABSTRACT
This study investigates the development of starch-based biodegradable plastic composites reinforced with kenaf fibre to improve mechanical performance and biodegradation. Starch was extracted from plant sources, and kenaf fibres were chemically treated prior to composite fabrication to improve interfacial compatibility. Composite films were produced from starch, glycerol, and varying kenaf fibre contents using optimized formulations derived from response surface methodology. Structural and physicochemical characterizations of the treated fibres and composites were conducted using Fourier transform infrared spectroscopy (FTIR) and X-ray diffraction (XRD) to evaluate functional group interactions and crystalline structures. Film density and water absorption were evaluated in accordance with ASTM D792 and ASTM D570, respectively, while chemical resistance was assessed in accordance with ASTM D543-95. Composite density ranged from 0.87 to 1.45 g/cm³, with higher values observed at increased kenaf fiber content, demonstrating the influence of formulation on composite structure. Film thickness ranged from 2.84 to 4.85 mm, with higher glycerol content increasing thickness and fiber addition contributing to improved dimensional uniformity. Mechanical testing showed that kenaf fiber reinforcement enhanced tensile strength to 22.91 MPa, elongation at break to 59.42%, and Young's modulus to 322.46 MPa. Water absorption measured according to ASTM D570 reached 85.20%, reflecting the hydrophilic nature of the starch matrix. Biodegradation studies using a soil burial method showed effective microbial degradation, with percentage weight loss ranging from 18.03% to 91.70%. Thermal analyses (DSC and TGA) revealed improved thermal stability for kenaf-reinforced composites, with crystallization and melting temperatures of approximately 250 °C and 340 °C, respectively. Overall, kenaf fiber reinforcement significantly enhanced the mechanical properties, thermal stability, chemical resistance, and biodegradability of starch-based bioplastics, highlighting their potential as sustainable alternatives to conventional plastics.

ARTICLE HISTORY
Received August 22, 2025
Accepted December 18, 2025
Published December 30, 2025

KEYWORDS
Starch-based biodegradable polymer composites, kenaf fibre, Mechanical properties, Soil burial, Thermal properties, Biochemical characteristics

INTRODUCTION
Plastics have become indispensable materials in modern society due to their versatility, durability, and low cost (AlMaadeed *et al.*, 2020; Hassan *et al.*, 2022; Badamasi and Salisu, 2025; Salisu *et al.*, 2025; Salisu and Ibrahim, 2024; Ibrahim *et al.*, 2024). However, their persistence in the environment and dependence on non-renewable petroleum resources have raised significant ecological concerns, particularly with regard to plastic waste accumulation and its long-term environmental impact (Elkaliny *et al.*, 2024; Hunter, 2024; Rajendran *et al.*, 2025). In response, global attention has shifted toward developing sustainable alternatives, particularly biodegradable plastics derived from renewable resources (Shen *et al.*, 2020; Thyavihalli Girijappa *et al.*, 2019). Among the various candidates, starch-based polymers have emerged as a promising option due to their abundance, biodegradability, and cost-effective (Dang *et al.*, 2025; Khoo *et al.*, 2023).

Despite these advantages, native starch-based plastics suffer from several limitations, including brittleness, poor mechanical strength, high water sensitivity, and low thermal stability (Agarwal et al., 2023). To overcome these drawbacks, reinforcement strategies using natural fibers have been explored, as they can significantly improve the structural integrity and mechanical performance of starch-based composites (Kibet *et al.*, 2025; Shaikh *et al.*, 2019). Natural fibers such as Kenaf, jute, sisal, and hemp are attractive reinforcements due to their biodegradability, low density, renewability, and favorable mechanical

Correspondence: Shehu Habibu. Department of Pure and Industrial Chemistry, Bayero University Kano, PMB 3011, Kano, Nigeria. ✉ shabibu.chm@buk.edu.ng.
How to cite: Sabo, D., Habibu, S., Ladan, M., Abdullahi, S., & Eric, D. (2025). Development of Starch-based Biodegradable Plastics reinforced with Natural Fiber for enhanced mechanical and biodegradation properties. *UMYU Scientifica*, 4(4), 338 – 358. https://doi.org/10.56919/usci.2544.030

properties (Kumar and Bedi, 2025; Nwuzor *et al.*, 2023). The integration of such fibers into starch matrices not only enhances mechanical strength but also supports biodegradation, aligning with sustainable material development goals (Çevik and Diambu, 2024; Farooq *et al.*, 2025).

Kenaf fibre, in particular, has attracted increasing research interest due to its high cellulose content, strong tensile strength, and availability as an agricultural by-product (Akil *et al.*, 2011; Motaung and Linganiso, 2018). Its incorporation into starch-based bioplastics has the potential to address the mechanical weaknesses of starch, providing composites with improved tensile strength, elongation at break, and thermal stability (García-Guzmán *et al.*, 2022; Gunawardene *et al.*, 2021). Furthermore, the addition of plasticizers, such as glycerol, can enhance flexibility, while the balance between starch, glycerol, and fibre content plays a crucial role in determining the composite's final properties (Abdel Hamid *et al.*, 2025; Cerqueira *et al.*, 2012).

Equally important is the biodegradation behavior of such composites. Since both starch and natural fibers are biodegradable (Thyavihalli Girijappa *et al.*, 2019), the resulting materials can undergo microbial degradation under natural environmental conditions, thereby reducing plastic pollution and supporting circular economy strategies (Jangong *et al.*, 2019; Oliver-Cuenca *et al.*, 2024; Sanyang *et al.*, 2015). However, the rate and extent of biodegradation are influenced by the composition of the composite, fiber-matrix interactions, and environmental conditions (Momeni *et al.*, 2023; Saha *et al.*, 2021). Understanding these interactions is essential for tailoring biodegradable plastics to specific applications ranging from packaging to agricultural films (Maraveas, 2020).

This study therefore focuses on the development of starch-based biodegradable plastics reinforced with natural fibres, with particular emphasis on kenaf fibre, to enhance both mechanical and biodegradation properties. The work aims to optimize material formulations by systematically varying starch, glycerol, and fibre content using response surface methodology and to investigate the structural, thermal, and mechanical properties of the composites. Characterization techniques such as Fourier Transform Infrared Spectroscopy (FTIR), Scanning Electron Microscopy, X-ray Diffraction (XRD), Differential Scanning Calorimetry (DSC), and Thermogravimetric Analysis (TGA) are used to evaluate interactions within the composites. By bridging material performance with environmental sustainability, this research contributes to the growing field of biodegradable materials, offering viable alternatives to petroleum-based plastics and supporting the transition toward greener industries.

MATERIAL AND METHODS

Materials

Reagents

All analytical-grade reagents were used as received, without further purification. The chemicals and materials employed in this study included sodium azide (98.0 %; Yicheng Fluoride, China), sodium hydroxide (99.0 %; Sigma-Aldrich, USA), glycerol (analytical grade; Hadis Group, Nigeria), and acetic acid (99.0 %; BP Chemicals, UK). Locally sourced and processed kenaf fibre, as well as locally sourced food-grade starch, were also used. Additional reagents included methyl red indicator (99.0 %; Sigma-Aldrich, USA), Kovac's reagent (96.0 %; Sigma-Aldrich, USA), Simmons citrate agar (99.0 %; Thermo Fisher Scientific, USA), and nutrient agar (98.0 %; HiMedia Laboratories, India). Barritt's reagents A and B (95.0 %; HiMedia Laboratories, India), hydrogen peroxide 30.0 % w/v; Evonik Industries AG, Germany), sodium hypochlorite 4.0% w/v; Olin Chemicals, USA), and potassium hydroxide (90.0 %; Hawkins, USA) were also used in the experimental procedures.

Methods

Extraction and preparation of starch from sweet potato

Potato starch was extracted according to the following method: sweet potato was bought from the market and soaked in distilled water with Sodium Azide (0.1 %) at a ratio of 1:2 for 24 hours to reduce microbial growth. Sweet potatoes were washed thoroughly, excess water drained, and the washed sweet potatoes were ground in a blender with sufficient water. The slurry was sieved. The remaining parts were slurred again with water to float off the germs and peels. The grinding, sieving, and regrinding of the potato particles were repeated multiple times until they were free of shaff. The starch was washed repeatedly by re-dispersing in distilled water and centrifuging until it appeared clean. The cleaned starch was air-dried on white paper for several days until completely dry. It was then blended to obtain a fine, white, powdery substance (Abotbina *et al.*, 2021).

Treatment of Kenaf Fibre *(Hibiscus Cannabinus)*

Treatment of Kenaf (Hibiscus cannabinus) was conducted using Kenaf fibre collected from Kibiya LGA, Kano State, Nigeria. The plant was washed and oven-dried at 30°C before being ground into powder using a blender. The treatment of Kenaf followed a four-step process: a) Acid treatment, (b)Alkaline treatment, and (c) Bleaching.

The dried and powdered Kenaf was immersed in a 0.2 M HCl solution at a 1:10 (weight/volume) ratio and stirred for 2 hours using a magnetic stirrer at 30°C. The resulting suspension was washed thoroughly with distilled water. The kenaf fibres were then stirred in a 5% NaOH solution at 80 ℃ using a magnetic stirrer for 3 hrs. This process was repeated three times and allowed to dry. Afterwards, bleaching was performed (Hazrol *et al.*, 2022b).

For bleaching, dried kenaf fibre was treated with a 10 % KOH solution at 80 °C for 3 hours, followed by multiple water washes, then treated with sodium hypochlorite (NaOCl) to effect bleaching, and the mixture was stirred at 75 °C. Hydrogen peroxide (H_2O_2) was used as a second bleaching agent at 75–85 °C for 70–75 minutes, after which it was washed with distilled water and allowed to dry for 24 Hrs (Hazrol *et al.*, 2022a).

Preparation of starch-based biodegradable polymers composite

The required amount of sweet potato starch given from the central composite design (CCD) table was dissolved in 100mL of distilled water and stirred continuously. The required amount of glycerol from the RSM table was added to the mixture and stirred continuously. The required amount of kenaf fibre was added to the mixture and stirred continuously. 1 mL of acetic acid was added to the mixture to balance the pH and achieve complete dispersion; the mixture was stirred continuously. The beaker containing the mixture was then placed on an electrical hotplate and was continuously stirred at 40 ℃ for 5 minutes. The suspension was transferred to a water bath at 85 ℃ for 15 minutes and continuous agitated with a glass rod. Gelatinization of the composite starts at 60 ℃ and yields a film-forming solution. The mixture was then poured into a glass mould and spread evenly. It was then allowed to dry at room temperature for 24-72 hours (Azmin *et al.*, 2024)

Fourier Transform Infrared Spectroscopy (FTIR)

Fourier transform infrared (FTIR) spectroscopy was used to assess possible changes in functional groups in the samples. The analysis was performed for each sample using an IR spectrometer (CARRY-630 Agilent spectrophotometer) at a resolution of 8 cm^{-1} over the range of 4000 to 500 cm^{-1} at the Instrumentation Lab of the Chemistry Department, Bayero University, Kano.

Film density

The density of the biodegradable composites was determined according to ASTM D792. The samples were cut into 2×4×3.2 mm, the mass was determined using a digital weighing balance, and the volume was measured using a micrometre screw gauge. These tests were performed three times for each biodegradable polymer composite sample, and the average values were used to evaluate the composite density, as reported by Draman et al. (2024). The density measurement (ϱ) was calculated using Equation 1.

$$\varrho = \frac{m}{v} \quad \text{.....(1)(Kumar } et\ al.\text{, 2025)}$$

Film Thickness

The thickness of each film sample was measured using a micrometre screw gauge (Mitutoyo Co., Kawasaki, Japan) with an accuracy of 0.001 mm from the Physics Lab of Bayero University, Kano. To ensure more reliable results, the thickness of each sample was measured five times at different areas of the film, and the mean film thickness was calculated (Abotbina *et al.*, 2021).

Water absorption test

The water absorption test was carried out in accordance with the ASTM D570 standard method for biodegradable composite, using an oven-dried test specimen. The biodegradable composite was weighed and immersed in water at ambient temperature for 24 hours. The specimens were removed, patted with a dry cloth, and then weighed using a digital weighing balance. This process was performed three times, and the average was used to evaluate the results. The dry weight before immersion (W initial) and the weight after immersion (W final) were noted. The water absorption (WA) percentage was then calculated using Equation (2) (Draman *et al.*, 2024).

$$\%\ \text{Water absorption} = \frac{w_2 - w_1}{w_1}\ x\ 100 \text{..... (2)}$$

Where w_1 = Initial weight and w_2= final weight

Biodegradation study (Soil burial Test)

The biodegradability test was carried out in order to measure the decrease in sample weight. The sample with a size (5cm x 5cm) was weighed as the initial weight and buried in a BUK biological garden in soil with a depth of 10 cm for 30 days. The sample weight was measured and observed on the 30th day. Equation (3) was used to calculate the weight reduction, where W_i is the initial sample weight (g) and W_2 is the final sample weight (g). Samples were taken from the soil, cleaned of residual soil using tissue, and weighed to measure the weight loss of the developed composite samples. The percentage weight loss of films during biodegradation was calculated by comparing the initial and final dry weight of the films before and after the soil burial test. The initial weight of the biodegradable composite films was determined after drying at 40°C for 24 hours to minimize any effect of moisture content on the films. The weight loss (%) was calculated using equation (3) (Abotbina *et al.*, 2021).

$$\%\ \text{Weight loss} = \frac{w_1 - w_2}{w_2}\ \text{x } 100 \text{ ..... (3)}$$

Where w_1 = initial weight and w_2 = final weight

Isolation and Identification of Biodegradable Composites Degrading Bacteria

Soil samples were processed using 0.9% saline to prepare suspensions, followed by serial dilution to reduce bacterial density. The diluted samples were inoculated on nutrient agar and incubated at 37°C for 48 hours. Distinct colonies were then sub-cultured to obtain pure isolates, which were characterized morphologically and biochemically using *Bergey's Manual of Determinative Bacteriology* (Afify and Biotechnology, 2025; Bergey, 1994).

Biochemical Tests

Indole Test

The indole test is a biochemical test that detects a bacterium's ability to produce indole as a metabolic

product of tryptophan. The isolate was inoculated in tryptone broth and incubated at 37 °C for 18-24 h, after which Kovac`s reagent (containing p-dimethylaminobenzaldehyde) was added to the broth. Positive result is indicated by the presence of a pink/red ring at the top-most layer of the broth, while a negative result is characterized by no color change(Afify and Biotechnology, 2025; Bergey, 1994).

Methyl Red Test

The Methyl Red test is a biochemical test that detects a bacterium's ability to produce stable mixed acids as metabolic end products of glucose metabolism. The isolate was inoculated in MR-VP broth and incubated at 37 °C for 24 h. After the incubation period few drops of methyl red indicator are added to the 24 h culture broth. Positive result is indicated with the culture broth change to red colour (pH ≤ 4.4) while Negative result shows a yellow/orange culture broth (pH ≥ 6.0) (Afify and Biotechnology, 2025; Bergey, 1994).

Voges Proskaeur Test

Voges-proskaeur test is a biochemical test that is utilized to detect bacterial ability to metabolize pyruvate into a neutral intermediate product called ácetylmethylcarbinol or 'ácetoin'. Using the same MR-VP 24 h broth culture as above. Barritts`s reagents (α-naphthol + KOH). Positive result is indicated by red/pink color change to the 24h broth culture, while a negative result shows no color change to the 24 h broth culture (Bergey, 1994).

Citrate utilization Test

The citrate utilization test is a biochemical test that detects a bacterium's ability to utilize citrate as its sole source of energy. The isolate was streaked on Simmons citrate agar (green at pH 6.9) and then incubated at 37 °C for 24 h. A positive result is characterized by agar colour change around the isolated streaks to a blue colour, while a negative result shows no colour change in the media (Afify and Biotechnology, 2025; Bergey, 1994).

Catalase Test

The catalase test is a simple procedure used to identify bacteria that produce the enzyme catalase, which decomposes hydrogen peroxide. It involves adding peroxide. It involves adding hydrogen peroxide to a bacterial culture and observing the immediate formation of bubbles, indicating the production of oxygen by the enzyme (Afify and Biotechnology, 2025; Bergey, 1994).

Oxidase Test

The oxidase test is a biochemical test used to identify bacteria that produce cytochrome oxidase, an enzyme involved in the electron transport chain. It's a simple test that can be performed by observing a color change after adding Kovac's reagent to the bacterial culture. A positive result indicates the presence of oxidase (dark purple or blue color), while a negative result indicates its absence (no color change) (Bergey, 1994).

Gram Staining

Gram staining was performed according to the method described by Afify and Biotechnology (2025) to differentiate bacterial isolates. A single colony from an overnight culture was smeared on a clean slide, air-dried, and heat-fixed. The smear was then sequentially stained with crystal violet (primary stain), treated with Gram's iodine (mordant), decolorized with ethyl alcohol, and counterstained with safranin. After air-drying, the slide was examined under a ×100 oil-immersion lens. This procedure enabled differentiation between Gram-positive and Gram-negative bacteria and provided insights into bacterial morphology, including cell shape, presence of flagella, and spores.

Chemical Resistivity Test

The chemical resistance tests of NaOH, Acetic acid, NaHCO3, and HCl were evaluated according to ASTM D 543-95. To determine the chemical absorbency, the samples were pre-weighed and thereafter immersed in the chemicals for 24 hours at ambient temperature. After 24 hours, the samples were removed from the chemicals, and the final weight of each sample was analyzed to determine the percentage weight gain, as represented in Equation (4) (Abotbina *et al.*, 2021).

$$\% \text{ Weight gain} = \frac{w_f - w_i}{w_i} \times 100 \quad \ldots\ldots\ldots\ldots\ldots\ldots\ldots\ldots (4)$$

Viscometric Measurement

Four different polymer samples of varying composition of 1 g, 0.8 g, 0.6 g, and 0.4 g were dissolved in 30 ml of 5% w/v NaOH. The solution was poured into a U-tube viscometer (U-tube viscometer type = Ubbelohde), and the time taken for the polymer solution to flow from the initial mark to the final mark was recorded. The process was carried out for all dissolved samples, and the flow time for the solvent and solute was recorded (Park *et al.*, 2023).

Mechanical Characterization

Tensile Properties

Tensile properties, including tensile strength, elongation at break, and Young's modulus, were measured using a universal testing machine (UTM) shimadzu (MODEL AG-1) at a speed of 10 mm/min in Mechanical Engineering Department, Bayero University, Kano, to assess the mechanical behavior of the different film samples. The tensile machine clamps were attached to a film strip (70 to 10 mm) that was pulled at a crosshead speed of 10 mm/min, with an effective grip distance of 30 mm. The machine was connected to computer software (Bluehill 3), which provided the mean of each parameter using five replicates of the tested sample. Equations 5 to 7 were used to calculate the values of tensile strength, Young's modulus, and elongation at break (Abotbina *et al.*, 2021).

$$\text{Tensile strength} = \frac{force}{Area} \quad \ldots\ldots\ldots\ldots\ldots\ldots\ldots\ldots\ldots (5)$$

$$\text{Strain} = \frac{Change\ in\ length}{Original\ length} \quad \ldots\ldots\ldots\ldots\ldots\ldots\ldots\ldots\ldots\ldots\ldots\ldots (\text{Kumar } et\ al., 2025)$$

$$\text{Young modulus} = \frac{Tensile\ strength}{Strain} \quad \ldots\ldots\ldots\ldots\ldots\ldots\ldots\ldots (7)$$

Thermal Analysis

Differential Scanning Calorimetry (DSC)

The DSC analysis of thin film samples was performed using a Mettler-Toledo DSC2 differential scanning calorimeter. The samples were heated at a controlled rate of 10 ℃ per minute under a nitrogen atmosphere using an aluminium pan. The experiment was conducted at a nitrogen flow rate of 100 ml/min and over a temperature range from 0 ℃ to 500 ℃ (Hazrol *et al.*, 2022a).

Thermogravimetric Analysis (TGA)

A thermogravimetric analysis (TGA) was performed using a TGA 4000 analyzer (Netherlands). A 10 mg sample was introduced into platinum crucibles under a nitrogen atmosphere and heated from room temperature to about 900 ℃ at 10 °C/min (Abotbina *et al.*, 2021).

X-Ray Diffraction (XRD)

XRD characterization of thin film samples was carried out using an X-ray Diffractometer, Thermoscientific model ARL'XTRA (SN 197492086). Approximately 2g of the sample was formed into a pellet and placed into the chamber of the machine. The sample was rotated at approximately 1.5 times the angular speed of the slit to maintain contact angle between the incident and reflected beams. The machine provides the phase distribution of biodegradable polymer composite recorded from Bragg's angle 10-70⁰ as conducted by Abotbina *et al.* (2021).

Scanning Electron Microscopy

Scanning electron microscopy was performed to examine the physical structure changes of the samples using a SEM model PhenomProX by phenomWorld, Eindhoven, The Netherlands. The sample was placed on a double-adhesive sample stub. The sample was coated with 5 nm of gold. Thereafter, it was taken to the chamber of the machine, where it was viewed via NaVCaM for focusing and minor adjustment. It was then transferred to SEM mode, focused, and brightness contrast was automatically adjusted. Afterwards, the morphologies at different magnifications were stored on a USB stick (Abotbina *et al.*, 2021).

Statistical analysis using response surface methodology (RSM)

A Central Composite Design from the statistical software Design-Expert Version 10 was used to optimize the composition for the preparation of the bio-composites. The ranges and levels of the factors (independent variables) investigated are shown in Table A. Three independent variables were employed, including Starch (A), Glycerol (B), and Kenaf fibre (C). The design consisted of 20 runs. The responses measured were tensile strength, elongation at break, and Young's modulus, as important parameters for sustainable packaging applications. Analysis of variance (ANOVA)was performed (Draman *et al.*, 2024).

Table A: Values and Levels of each independent variable in Central Composite Design.

Variables	Levels	
	Low level (-1)	High level (+1)
Starch(g)	30.81	36.65
Glycerol(ml)	12	17
Fibre(g)	0	4.42

RESULTS AND DISCUSSIONS

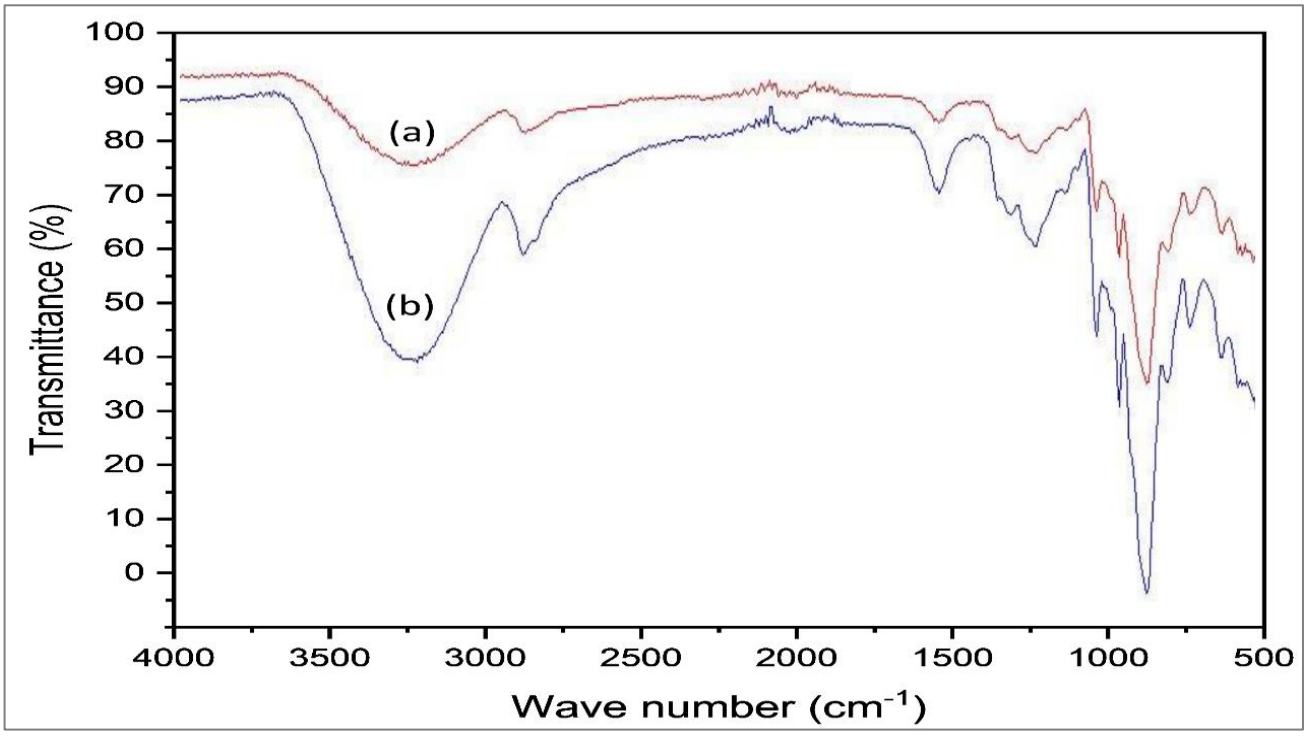

Figure 1: FTIR Spectra of commercial starch (a) and extracted starch (b)

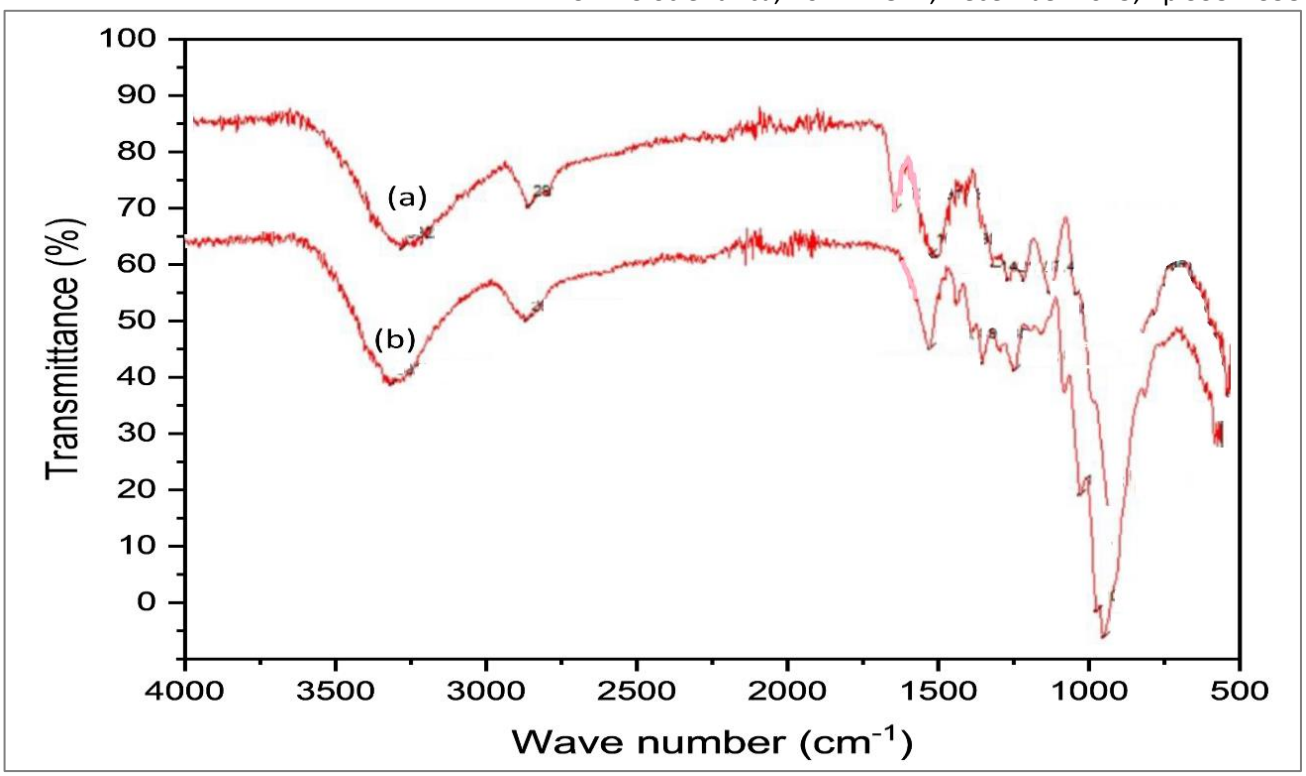

Figure 2: FTIR Spectra of untreated (a) and treated (b) kenaf fibres

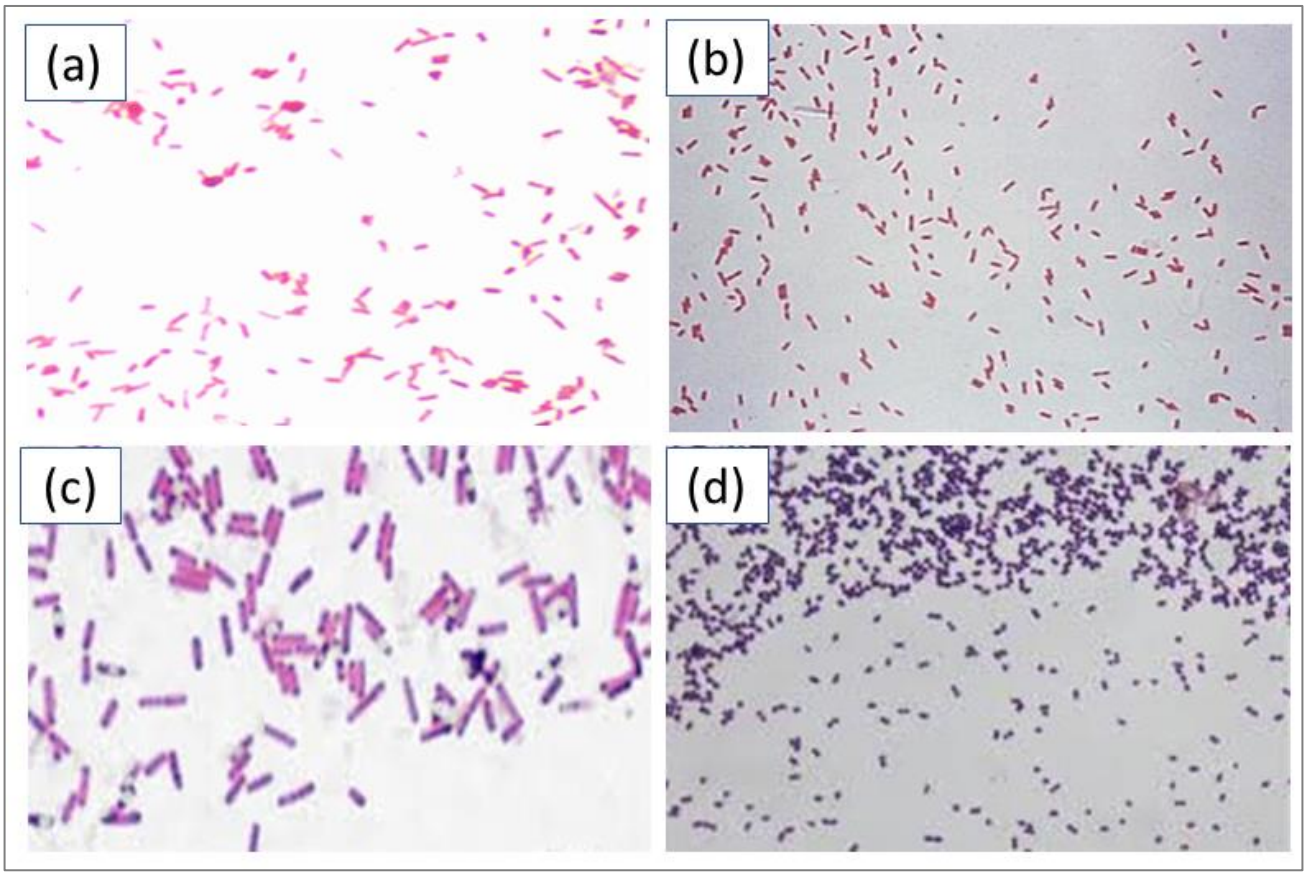

Figure 3: Staining of bacteria under microscope (a) *Enterobacter* sp under ×100 magnification, (b) *Pseudomonas* sp under ×100 magnification, (c) *Bacillus* sp under ×100 magnification, (d) *Enterococcus* sp under ×100 magnification

The FTIR spectra of extracted and commercial starch display similar characteristic bands, confirming comparable molecular structures (Figure 1). Both samples exhibited broad O–H stretching vibrations around 3300–3400 cm^{-1} and C=O and C–O stretching peaks near 1200 cm^{-1} and 1150–1000 cm^{-1}, respectively, indicating the presence of hydroxyl and glycosidic linkages typical of starch (Hazrol et al., 2022a). These similarities suggest that the extracted starch maintains the core structural features of commercial starch, making it a viable

substitute. However, slight variations in peak intensity and position, particularly around 1600–1700 cm^{-1}, imply minor structural or compositional differences likely resulting from the extraction process, which may affect its functional performance (Abdel Hamid *et al.*, 2025).

The FTIR spectra of untreated and treated kenaf fibers reveal clear chemical and structural differences. In the untreated fiber, peaks at 3322 cm^{-1} (O–H stretching) and 2915 cm^{-1} (C–H stretching) indicate the presence of hydroxyl and aliphatic groups from cellulose, hemicellulose, and lignin (Figure 2). The band at 1596 cm^{-1} corresponds to aromatic C=C stretching in lignin, while peaks near 1100 cm^{-1} represent C–O stretching, confirming the fiber's complex natural composition.

After treatment, notable spectral changes occurred; the reduced intensity of the O–H band (3328 cm^{-1}) and the diminished aromatic peak (1592 cm^{-1}) suggest partial removal of hemicellulose and lignin. The more pronounced C–O stretching peak around 1030 cm^{-1} indicates greater cellulose exposure. The treatment effectively modified the chemical structure of kenaf fibre, improving its suitability as a reinforcement material in starch-based biodegradable composites (Hazrol *et al.*, 2022a).

Density of biodegradable polymer composite

The density of the biodegradable polymer composites was measured, and the results are given in Table 1.

Table 1: Density Analysis of Biodegradable Polymer Composites

S/N	Starch Content (g)	Glycerol Content (ml)	Fibre Content (g)	Density (g/cm^3)
1	33.75	12.00	1.65	1.13
2	32.00	13.00	3.30	1.28
3	36.69	14.50	1.65	1.16
4	33.75	14.50	1.65	1.15
5	33.75	14.50	1.65	1.14
6	35.5	13.00	3.30	1.26
7	32.00	16.00	0.00	0.91
8	32.00	13.00	0.00	0.87
9	33.75	14.50	1.65	1.16
10	32.00	16.00	3.30	1.27
11	30.81	14.50	1.65	1.12
12	35.50	16.00	3.30	1.30
13	35.50	13.00	0.00	0.92
14	33.75	17.00	1.65	1.13
15	33.75	14.50	1.65	1.17
16	35.50	16.00	0.00	0.93
17	33.75	14.50	1.65	1.14
18	33.75	14.50	1.65	1.15
19	33.75	14.50	1.00	1.10
20	33.75	14.50	4.42	1.45

The density analysis of the biodegradable composite reveals a diverse range of densities, influenced by varying starch, glycerol, and fibre contents. Notably, the highest density recorded was 1.45 g/cm^3 for a sample with 33.75 g of starch, 14.5 ml of glycerol, and 4,42 g of fiber. This suggests a significant interaction between these components, potentially enhancing the structural integrity of the biodegradable composite several samples exhibited notably lower densities, such as the one with 0 g of fiber, which recorded a density of 0.87 g/cm^3. This indicates that fibre content enhances density, likely by influencing the composite's porosity and mechanical properties (Danasabe and Stephen, 2018).

Thickness analysis

The thickness of the biodegradable polymer composites was determined, and the results were presented in Table 2.

Table 2: Result of Thickness Analysis of Biodegradable Polymer Composite

S/N	Starch Content (g)	Glycerol Content (ml)	Fibre Content (g)	Thickness (mm)
1	33.75	12.00	1.65	3.59
2	32.00	13.00	3.30	4.09
3	36.69	14.50	1.65	3.93
4	33.75	14.50	1.65	4.33
5	33.75	14.50	1.65	4.29
6	35.5	13.00	3.30	4.13
7	32.00	16.00	0.00	4.85
8	32.00	13.00	0.00	4.54
9	33.75	14.50	1.65	4.21
10	32.00	16.00	3.30	4.14
11	30.81	14.5.0	1.65	3.63
12	35.50	16.00	3.30	4.04
13	35.50	13.00	0.00	2.84
14	33.75	17.00	1.65	3.00
15	33.75	14.50	1.65	3.17
16	35.50	16.00	0.00	3.55
17	33.75	14.50	1.65	3.38
18	33.75	14.50	1.65	4.12
19	33.75	14.50	1.00	3.57
20	33.75	14.50	4.42	4.17

The thickness of the biodegradable polymer composites ranged from 2.84 mm to 4.85 mm, primarily influenced by the proportions of starch, glycerol, and fibre. Samples with higher glycerol content, particularly those without fiber, exhibited greater thickness due to increased mixture viscosity. In contrast, incorporating kenaf fiber generally reduced thickness, suggesting its role in densifying the composite matrix. Samples containing moderate fiber levels (≈1.65 g) maintained more consistent thickness around 4 mm, whereas fibre-free samples showed higher variability. These results highlight the need to optimize

the ratios of starch, glycerol, and fibre to achieve uniform, application-specific thickness in the production of biodegradable composites (Spiridon *et al.*, 2015).

Water absorption of biodegradable polymer composite

The water absorption analysis of the biodegradable polymer composites was conducted to determine the percentage water absorption, and the results are given in Table 3.

Water absorption in the biodegradable polymer composites varied significantly with changes in starch, glycerol, and fiber composition. The highest absorption (85.20%) occurred in samples with high starch and glycerol content, reflecting strong hydrophilicity due to abundant hydroxyl groups. In contrast, samples with lower starch or fiber content, such as Sample 19 (39.21%), showed reduced water uptake, suggesting that kenaf fiber contributes to structural stability and limits moisture penetration (Draman *et al.*, 2024). Moreover, increased glycerol levels tended to decrease water absorption by forming a more cohesive, less porous matrix (Dan-Asabe *et al.*, 2019). Generally, the results emphasize the need to balance the ratios of starch, glycerol, and fibre to optimize moisture resistance and mechanical performance in biodegradable composites.

Table 3: Water Absorption of Biodegradable Polymer Composite

S/N	Starch Content (g)	Glycerol Content (ml)	Fibre Content (g)	Initial weight (W_1)	Final weight (W_F)	Water absorption (%)
1	33.75	12.00	1.65	5.10	8.20	60.80
2	32.00	13.00	3.30	5.90	9.10	54.23
3	36.69	14.50	1.65	6.50	9.80	50.80
4	33.75	14.50	1.65	5.71	9.30	62.90
5	33.75	14.50	1.65	7.10	10.60	49.30
6	35.50	13.00	3.30	6.58	10.90	65.70
7	32.00	16.00	0.00	4.90	7.80	59.20
8	32.00	13.00	0.00	6.80	10.40	52.94
9	33.75	14.50	1.65	5.20	9.63	85.20
10	32.00	16.00	3.30	5.13	9.24	80.12
11	30.81	14.50	1.65	6.00	9.98	66.33
12	35.50	16.00	3.30	5.38	8.95	66.36
13	35.50	13.00	0.00	6.28	10.00	59.24
14	33.75	17.00	1.65	4.48	7.65	70.80
15	33.75	14.50	1.65	7.68	11.00	43.23
16	35.50	16.00	0.00	5.37	8.89	65.60
17	33.75	14.50	1.65	7.22	11.22	55.40
18	33.75	14.50	1.65	7.00	11.00	57.14
19	33.75	14.50	1.00	8.62	12.00	39.21
20	33.75	14.50	4.42	5.68	8.99	58.30

Biodegradation studies of biodegradable polymer composites

Biodegradation studies of the biodegradable polymer composites were conducted to determine weight loss (%), and the results are presented in Table 4.

Biodegradation tests of the starch-based polymer composites showed weight losses ranging from 18.03% to 91.70%, depending on the material composition. The highest degradation (91.70%) occurred in samples with higher starch and glycerol content, indicating that these components enhance microbial activity by increasing the availability of degradable organic matter (Ahmad *et al.*, 2014). Conversely, composites with higher fibre content exhibited lower biodegradation rates, suggesting that kenaf fibre enhances structural stability and resistance to microbial attack. Overall, the findings highlight the need to optimize the ratios of starch, glycerol, and fibre to achieve balanced biodegradability and mechanical performance in sustainable composite materials (Draman et al., 2024).

The soil samples yielded 4 isolates. This observation may be due to the fact that biodegradable polymer composite-degrading bacteria are present in the soil. This indicates that the isolates can utilize the biopolymer and hence degrade it. The isolates were found to possess the degradation capability after 30 days of soil burial. Four isolates were selected from the nutrient agar plate after 48 hours of incubation. The isolates were then subjected to morphological and biochemical identification. The isolates were identified as Gram-positive and Gram-negative bacteria based on their biochemical

characteristics, as shown in Table 5. The results show that diverse bacterial species in the soil can utilize the biopolymer as a substrate and degrade it (Afify and Biotechnology, 2025).

The isolates were then subjected to different morphological, biochemical and molecular identification. The four isolates were identified as two Gram-positive and two Gram-negative bacteria. Then, based on biochemical characterizations (Figure 3), it was provisionally identified as *Bacillus sp.*, *Enterococcus sp.*, *Enterobacter sp.*, and *Pseudomonas sp.*, respectively (Afify and Biotechnology, 2025).

Table 4: Biodegradation Studies of Biodegradable Polymer Composite

S/N	Starch Content (g)	Glycerol Content (ml)	Fibre Content (g)	Initial weight (W_i)	Final Weight (W_f)	Weight loss (%)
1	33.75	12.00	1.65	4.80	0.40	91.70
2	32.0	13.00	3.30	2.50	0.60	76.00
3	36.69	14.50	1.65	4.80	2.80	41.70
4	33.75	14.50	1.65	3.20	2.60	18.80
5	33.75	14.50	1.65	2.80	1.50	46.40
6	35.50	13.00	3.30	8.10	4.70	42.00
7	32.00	16.00	0.00	5.10	3.75	26.50
8	32.00	13.00	0.00	5.60	4.30	23.20
9	33.75	14.50	1.65	4.90	3.10	36.70
10	32.00	16.00	3.30	6.60	1.20	81.82
11	30.81	14.50	1.65	7.50	5.40	28.00
12	35.50	16.00	3.30	11.10	4.20	62.20
13	35.50	13.00	0.00	4.80	2.00	58.33
14	33.75	17.00	1.65	9.80	2.70	72.50
15	33.75	14.50	1.65	10.20	2.90	71.60
16	35.50	16.00	0.00	12.40	3.00	75.81
17	33.75	14.50	1.65	7.10	0.80	88.73
18	33.75	14.50	1.65	6.60	4.00	39.40
19	33.75	14.50	1.00	10.00	7.90	21.00
20	33.75	14.50	4.42	6.10	5.00	18.03

Chemical resistivity analysis

The effects of hydrochloric acid, acetic acid, and sodium hydrogen carbonate on the biodegradable composites were studied to assess their behaviour toward the acids and alkali used. The weight gain (%) was determined, and the results are presented in Table 6, 7, and 8, respectively.

Chemical absorbency analysis in 10% HCl revealed weight gain values ranging from 10% to 90% among the biodegradable composites, depending on composition. Samples containing higher starch and glycerol levels (e.g., 32 g starch, 13–14.5 ml glycerol) exhibited the highest weight gain (90%), indicating strong hydrophilic and acid-absorbent characteristics due to the polar nature of these components (Jadhav *et al.*, 2023). Conversely, composites with higher kenaf fibre content showed reduced absorbance, as fibre rigidity limits interaction with acidic media. These results emphasize that adjusting the ratios of starch, glycerol, and fibre is essential for tailoring chemical resistance in biodegradable composites, especially for applications requiring acid tolerance or controlled chemical interactions.

The chemical-resistivity test using 5% $NaHCO_3$ showed weight gains ranging from 15% to 90% across the biodegradable composite samples. The highest gain (90%) occurred in the sample containing 33.75 g starch, 14.5 ml glycerol, and 1.65 g fibre, indicating a strong interaction with the alkaline medium due to the hydrophilic nature of starch and glycerol. In contrast, samples with higher fibre content exhibited lower weight gains (as low as 15%), suggesting that fibre reduces surface interactions and absorption capacity. These results demonstrate that starch and glycerol enhance the composite's affinity for basic environments, while fiber content influences chemical resistance. Optimizing their ratios is therefore essential for tailoring composite performance in applications that require alkaline stability (Jadhav *et al.*, 2023).

Chemical absorbency analysis using 5% acetic acid showed weight gains ranging from 21.10% to 91.00% across the biodegradable composite samples. The highest gain (91.00%) was recorded for the sample containing 33.75 g starch, 14.5 ml glycerol, and 1.65 g fibre, indicating a strong interaction with acetic acid due to the hydrophilic nature of starch and glycerol.

Table 5: Biochemical characteristics of isolated bacteria

Isolates	Biochemical analysis	Characteristics	Organism
Isolate 1	Gram reaction	-	*Enterobacter sp.*
	Methyl red	-	
	Voges proskaeur	+	
	Citrate	+	
	Oxidase	-	
	Catalase	+	
	Indole	-	
Isolate 2	Gram reaction	-	*Pseudomonas sp.*
	Methyl red	+	
	Voges proskaeur	-	
	Citrate	+	
	Oxidase	+	
	Catalase	+	
	Indole	-	
Isolate 3	Gram reaction	+	*Bacillus sp.*
	Methyl red	-	
	Voges proskaeur	+	
	Citrate	+	
	Oxidase	-	
	Catalase	+	
	Indole	-	
Isolate 4	Gram reaction	+	*Enterococcus sp*
	Methyl red	-	
	Voges proskaeur	+	
	Citrate	-	
	Oxidase	-	
	Catalase	-	

Key: + and − indicates positive and negative result.

Table 6: Chemical resistivity analysis using 10% HCl

S/N	Starch Content (g)	Glycerol Content (m)l	Fibre Content (g)	Initial weight W_i(g)	Final weight W_f(g)	Weight gain (%)
1	33.75	12.00	1.65	1.00	1.70	70
2	32.00	13.00	3.30	1.00	1.90	90
3	36.69	14.50	1.65	1.00	1.80	80
4	33.75	14.50	1.65	1.00	1.80	80
5	33.75	14.50	1.65	1.00	1.40	40
6	35.50	13.00	3.30	1.00	1.20	20
7	32.00	16.00	0.00	1.00	1.50	50
8	32.00	13.00	0.00	1.00	1.70	70
9	33.75	14.50	1.65	1.00	1.60	60
10	32.00	16.00	3.30	1.00	1.40	40
11	30.81	14.50	1.65	1.00	1.30	30
12	35.50	16.00	3.30	1.00	1.30	30
13	35.50	13.00	0.00	1.00	1.50	50
14	33.75	17.00	1.65	1.00	1.30	10
15	33.75	14.50	1.65	1.00	1.10	10
16	35.50	16.00	0.00	1.00	1.80	80
17	33.75	14.50	1.65	1.00	1.70	70
18	33.75	14.50	1.65	1.00	1.90	90
19	33.75	14.50	1.00	1.00	1.70	70
20	33.75	14.50	4.42	1.00	1.40	40

Table 7: Chemical resistivity analysis using 5% $NaHCO_3$

S/N	Starch Content (g)	Glycerol Content (ml)	Fibre Content (g)	Initial weight (g)	Final weight (g)	Weight gain (%)
1	33.75	12.00	1.65	1.00	1.65	65
2	32.00	13.00	3.30	1.00	1.84	84
3	36.69	14.50	1.65	1.00	1.79	79
4	33.75	14.50	1.65	1.00	1.56	56
5	33.75	14.50	1.65	1.00	1.22	22
6	35.50	13.00	3.30	1.00	1.43	43
7	32.00	16.00	0.00	1.00	1.46	46
8	32.00	13.00	0.00	1.00	1.68	68
9	33.75	14.50	1.65	1.00	1.73	73
10	32.00	16.00	3.30	1.00	1.39	39
11	30.81	14.50	1.65	1.00	1.31	31
12	35.50	16.00	3.30	1.00	1.29	29
13	35.50	13.00	0.00	1.00	1.49	49
14	33.75	17.00	1.65	1.00	1.28	28
15	33.75	14.50	1.65	1.00	1.15	15
16	35.50	16.00	0.00	1.00	1.79	79
17	33.75	14.50	1.65	1.00	1.72	72
18	33.75	14.50	1.65	1.00	1.90	90
19	33.75	14.50	1.00	1.00	1.70	70
20	33.75	14.50	4.42	1.00	1.42	42

Table 8: Chemical resistivity analysis using 5% Acetic acid

S/N	Starch Content (g)	Glycerol Content (ml)	Fibre Content (g)	Initial weight (g)	Final weight (g)	Weight gain (%)
1	33.75	12.00	1.65	1.00	1.635	63.50
2	32.00	13.00	3.30	1.00	1.880	88.00
3	36.69	14.50	1.65	1.00	1.800	80.00
4	33.75	14.50	1.65	1.00	1.830	83.00
5	33.75	14.50	1.65	1.00	1.480	48.00
6	35.50	13.00	3.30	1.00	1.300	30.00
7	32.00	16.00	0.00	1.00	1.400	40.00
8	32.00	13.00	0.00	1.00	1.621	62.10
9	33.75	14.50	1.65	1.00	1.610	61.00
10	32.00	16.00	3.30	1.00	1.340	34.00
11	30.81	14.50	1.65	1.00	1.320	32.00
12	35.50	16.00	3.30	1.00	1.320	32.00
13	35.50	13.00	0.00	1.00	1.510	51.00
14	33.75	17.00	1.65	1.00	1.285	28.50
15	33.75	14.50	1.65	1.00	1.211	21.10
16	35.50	16.00	0.00	1.00	1.810	81.00
17	33.75	14.5	1.65	1.00	1.682	68.20
18	33.75	14.5	1.65	1.00	1.910	91.00
19	33.75	14.5	1.00	1.00	1.721	72.10
20	33.75	14.5	4.42	1.00	1.490	49.00

Table 9: Viscosity data for the Biodegradable polymer composite material at 30 ℃

Sample	Sample weight (g)	Concentration (gdL^{-1})	t(s)	η_{rel}	η_{sp}	η_{red}	η_{inh}
1	1.0	3.33	14.80	4.205	3.205	0.962	0.413
	0.8	2.67	11.60	3.295	2.295	0.850	0.447
	0.6	2.00	8.00	2.273	1.273	0.637	0.411
	0.4	1.33	6.50	1.847	0.847	0.637	0.461
8	1.0	3.33	33.00	9.375	8.375	2.515	0.672
	0.8	2.67	27.60	7.841	6.841	2.562	0.771
	0.6	2.00	20.00	5.682	4.682	2.341	0.869
	0.4	1.33	9.33	2.651	1.651	1.241	0.733
16	1.0	3.33	20.65	5.866	4.866	1.461	0.531
	0.8	2.67	14.30	4.063	3.063	1.461	0.525
	0.6	2.00	9.10	2.585	1.585	0.793	0.475
	0.4	1.33	5.23	1.486	0.486	0.365	0.298
10	1.0	3.33	36.90	10.483	9.483	2.848	0.706
	0.8	2.67	12.50	3.551	2.551	0.955	0.475
	0.6	2.00	9.70	2.756	1.756	0.878	0.507
	0.4	1.33	6.58	1.869	0.869	0.653	0.470

Table 10: Response Surface Methodology

Run	Factor 1 A:Starch Content (g)	Factor 2 B:Glycerol Content (ml)	Factor 3 C:Fibre Content (g)	Response 1 Tensile Strength (Mpa)	Response 2 Elongation at Break (%)	Response 3 Young Modulus (Mpa)
1	33.75	12.00	1.65	2.00	38.98	84.40
2	32.00	13.00	3.30	5.05	26.07	19.37
3	36.69	14.50	1.65	6.14	16.04	111.64
4	33.75	14.50	1.65	4.41	18.99	31.52
5	33.75	14.50	1.65	3.05	24.66	41.87
6	35.50	13.00	3.30	22.91	5.15	322.46
7	32.00	16.00	0.00	10.50	11.66	168.02
8	32.00	13.00	0.00	2.09	59.42	3.52
9	33.75	14.50	1.65	0.45	15.51	2.90
10	32.00	16.00	3.30	2.05	23.71	6.29
11	30.81	14.50	1.65	2.23	9.93	22.44
12	35.50	16.00	3.30	3.00	48.77	5.41
13	35.50	13.00	0.00	4.14	29.16	14.18
14	33.75	17.00	1.65	3.77	26.97	20.65
15	33.75	14.50	1.65	5.82	18.99	41.99
16	35.50	16.00	0.00	5.73	18.88	30.34
17	33.75	14.50	1.65	3.36	16.98	41.62
18	33.75	14.50	1.65	2.36	24.75	9.55
19	33.75	14.50	1.00	5.73	19.11	33.25
20	33.75	14.50	4.42	6.18	18.51	94.22

Conversely, samples with higher fibre content, such as those containing 4.42 g fibre, exhibited lower absorbance (49%), suggesting that increased fibre reduces porosity and limits acid penetration. These results demonstrate that adjusting the ratios of starch, glycerol, and fibre is essential for optimising chemical resistance in acidic environments, aligning with findings by Jadhav et al. (2023).

Table 11: Analysis of Variance Result for Tensile Strength Response

Source	Term df	Error df	F	p-value Prob> F	
Subplot	9	10.00	5.07	0.0091	Significant
A-Starch Content	1	10.00	4.87	0.0519	
B-Glycerol Content	1	10.00	0.95	0.3535	
C-Fibre Content	1	10.00	0.47	0.5071	
AB	1	10.00	9.11	0.0129	
AC	1	10.00	7.50	0.0209	
BC	1	10.00	17.51	0.0019	
A^2	1	10.00	0.92	0.3607	
B^2	1	10.00	0.12	0.7397	
C^2	1	10.00	2.59	0.1387	

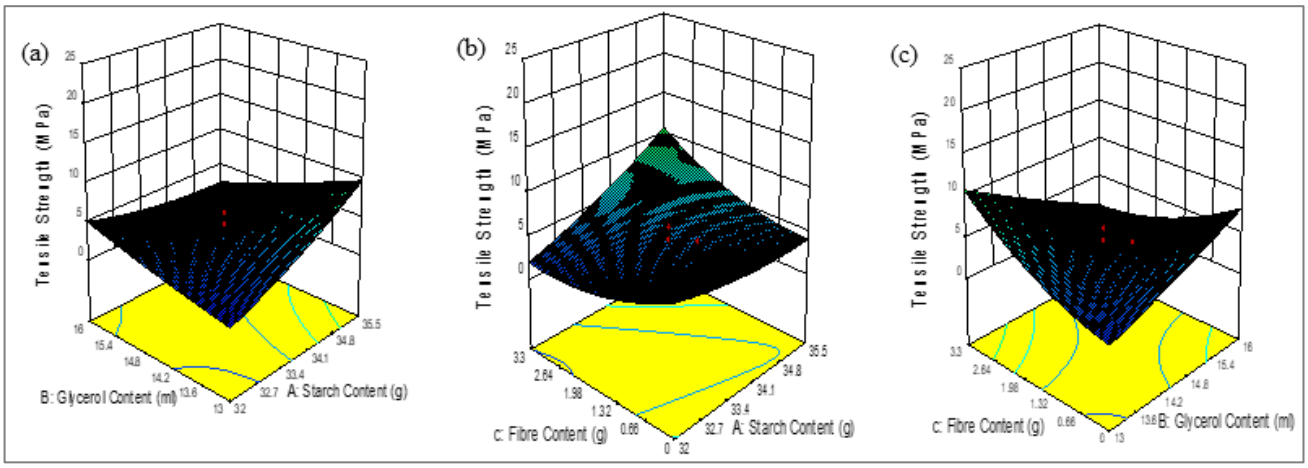

Figure 4: The effect of (a) glycerol and starch content, (b) Fibre and Starch content, (c) Fibre and glycerol content interaction on tensile strength.

Table 12: Analysis of Variance Result for Elongation at Break Response

Source	Term df	Error df	F	p-value Prob> F	
Subplot	9	6.40	15.84	0.0012	Significant
A-Starch Content	1	7.68	0.27	0.6185	
B-Glycerol Content	1	7.68	4.92	0.0587	
C-Fibre Content	1	8.67	2.87	0.1258	
AB	1	7.68	42.88	0.0002	
AC	1	7.68	4.55	0.0669	
BC	1	7.68	60.70	< 0.0001	
A^2	1	9.81	1.29	0.2826	
B^2	1	9.84	12.05	0.0062	
C^2	1	5.79	1.73	0.2382	

Viscometric analysis

The viscosities of the biodegradable plastic composites were measured, and the relative, specific, reduced, and inherent viscosities were evaluated and are presented in Table 9.

NB: 1: Sample with fibre, 8: Sample without fibre, 16: Sample without fibre , 10: Sample with fibre

Viscosity analysis at 30°C revealed that the biodegradable polymer composite's viscosity parameters—relative (η_{rel}), specific (η_{sp}), reduced (ηred), and inherent (η_{inh}) increase with concentration, indicating stronger molecular interactions at higher sample weights. The relative viscosity increased from 3.295 to 4.205 as the concentration increased from 2.67 g/dL to 3.33 g/dL, confirming that denser solutions exhibit greater resistance to flow. Sample 8 showed the highest reduced viscosity (2.515), suggesting enhanced polymer chain interactions that could improve the mechanical strength of solid composites. These findings demonstrate that viscosity behaviour is closely linked to molecular structure and

concentration, providing valuable insights for optimising biodegradable composite formulations for industrial applications such as coatings and adhesives (Koltzenburg et al., 2017).

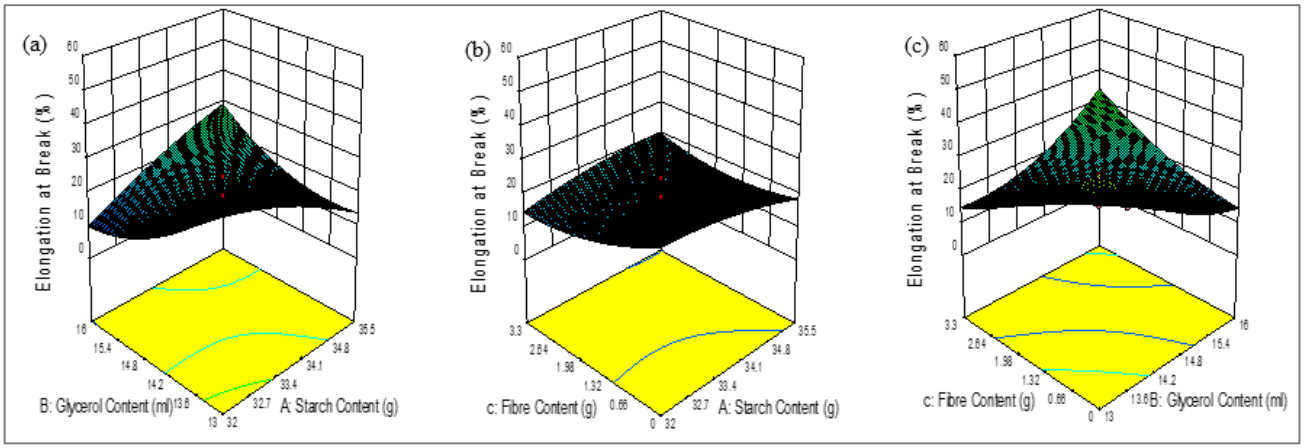

Figure 5: **The effect of (a) Glycerol and Starch content, (b) Fibre and Starch content, and (c)Fibre and glycerol content interaction on Elongation at break.**

Table 13: Analysis of Variance (ANOVA) for Young Modulus Response

Source	Term df	Error df	F	p-value Prob> F	
Subplot	9	10.00	23.98	< 0.0001	Significant
A-Starch Content	1	10.00	15.97	0.0025	
B-Glycerol Content	1	10.00	9.95	0.0103	
C-Fibre Content	1	10.00	4.52	0.0594	
AB	1	10.00	52.73	< 0.0001	
AC	1	10.00	47.49	< 0.0001	
BC	1	10.00	67.25	< 0.0001	
A^2	1	10.00	6.14	0.0326	
B^2	1	10.00	2.56	0.1404	
C^2	1	10.00	4.45	0.0611	

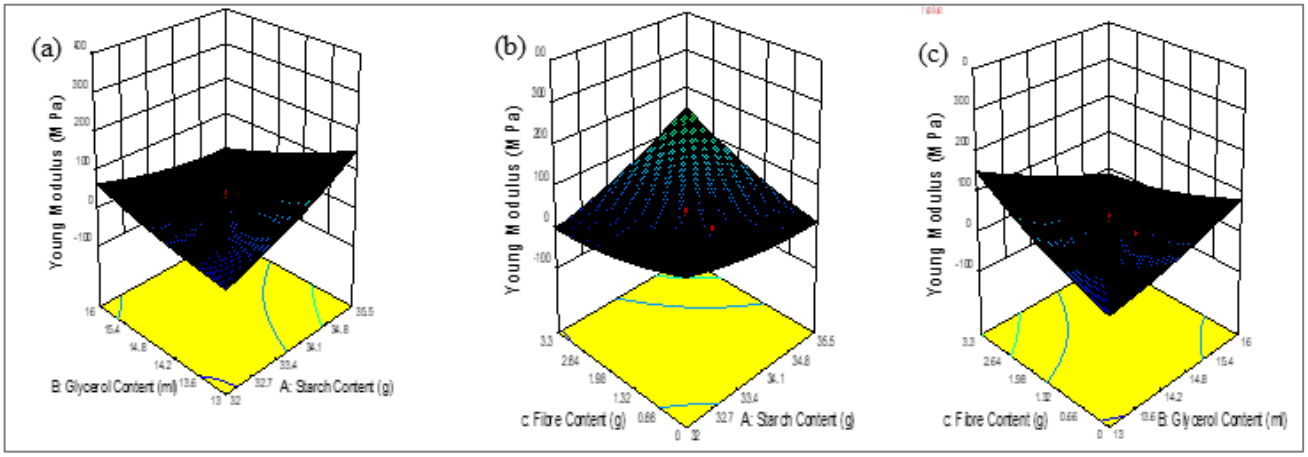

Figure 6: **The effect of (a) Starch and Glycerol content,(b) Fibre and Starch content, (c) Fibre and glycerol content interaction on Young's modulus.**

Mechanical charactization

The software suggested values for Starch, Glycerol and Fiber content. The responses were measured and entered in the table. The results presented in Table 10 indicate the mechanical properties of the prepared biodegradable polymer composites.

The Central Composite Design (CCD) analysis demonstrated that variations in starch, glycerol, and fiber content significantly influence the mechanical properties of the biodegradable composites. The highest tensile strength (22.91 MPa) was obtained in Sample 6, indicating optimal component interaction and improved load-

bearing capacity. Maximum elongation at break (59.42%) occurred in Sample 12, reflecting enhanced flexibility and ductility. Young's modulus values, reaching up to 322.46 MPa, highlighted the potential for achieving high stiffness through formulation adjustments. Overall, the results confirm that balancing the ratios of starch, glycerol, and fibre is key to tailoring mechanical performance for targeted applications, such as packaging and structural materials, aligning with the findings of Draman et al. (2024).

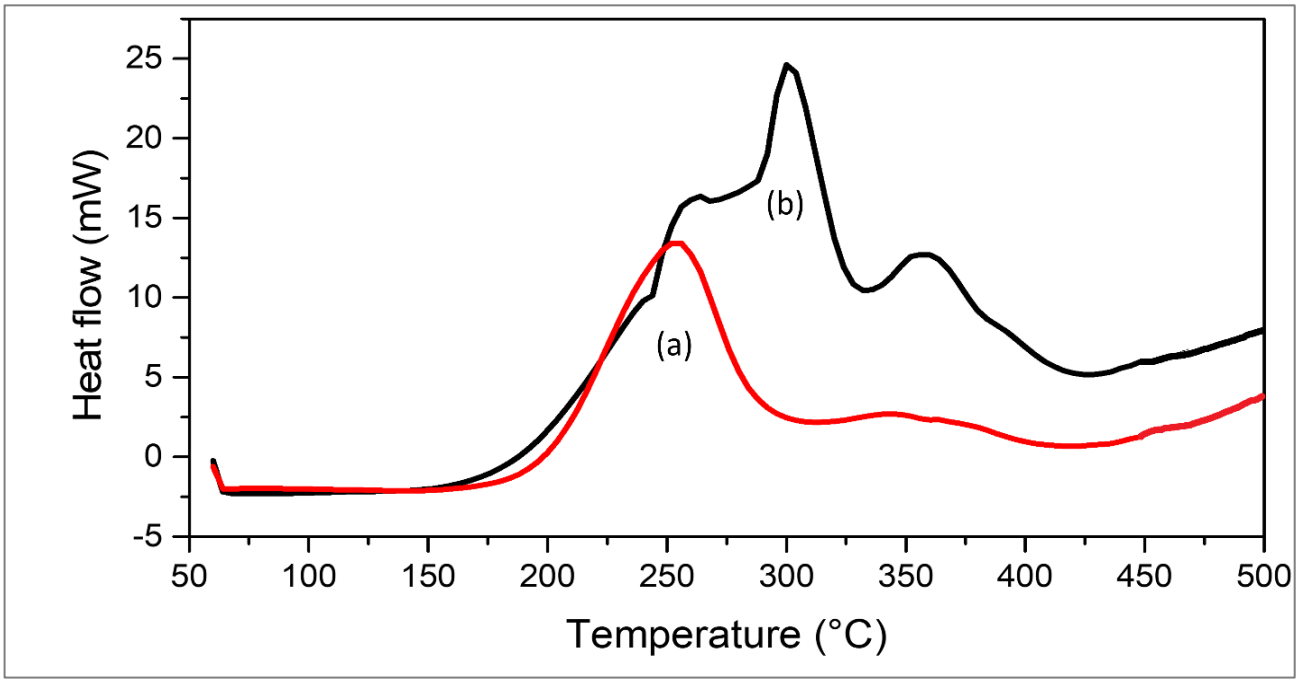

Figure 7: DSC Thermogram of biodegradable composite with (a), and without kenaf fibre (b)

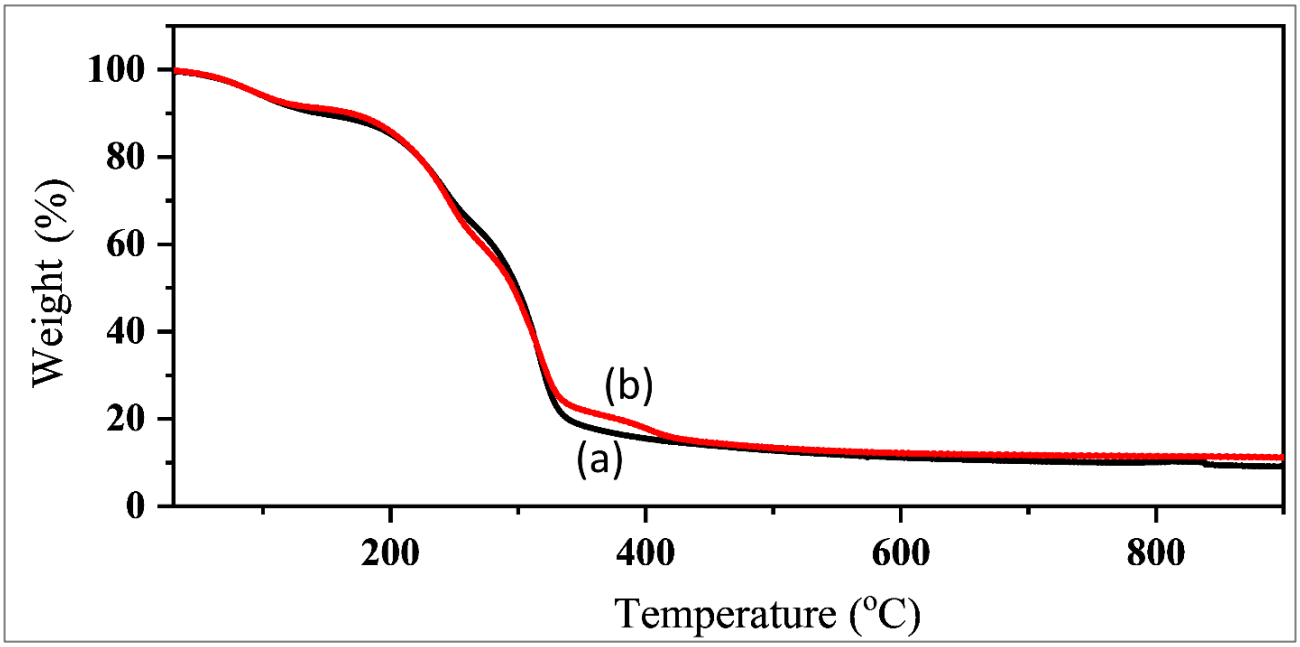

Figure 8: TGA result of biodegradable composite with (a), and without kenaf fibre (b)

ANOVA results from the response surface analysis revealed that starch, glycerol, and fiber interactions significantly affect the tensile strength of the biodegradable composites (Table 11). A p-value of 0.0091 confirmed the overall model's significance, with interaction terms AB (starch–glycerol), AC (starch–fiber), and BC (glycerol–fiber) showing strong effects ($p = 0.0129$, 0.0209, and 0.0019, respectively). While the effects of glycerol and fibre alone were not significant, their interactions with starch significantly influenced tensile performance. The regression model indicated that starch positively contributes to tensile strength, whereas excessive glycerol reduces it. Positive interaction coefficients for AC and BC suggest synergistic effects that enhance strength when components are optimally combined. These findings emphasize the need to optimize component interactions rather than individual concentrations to achieve superior mechanical performance in biocomposite materials (Draman et al., 2024).

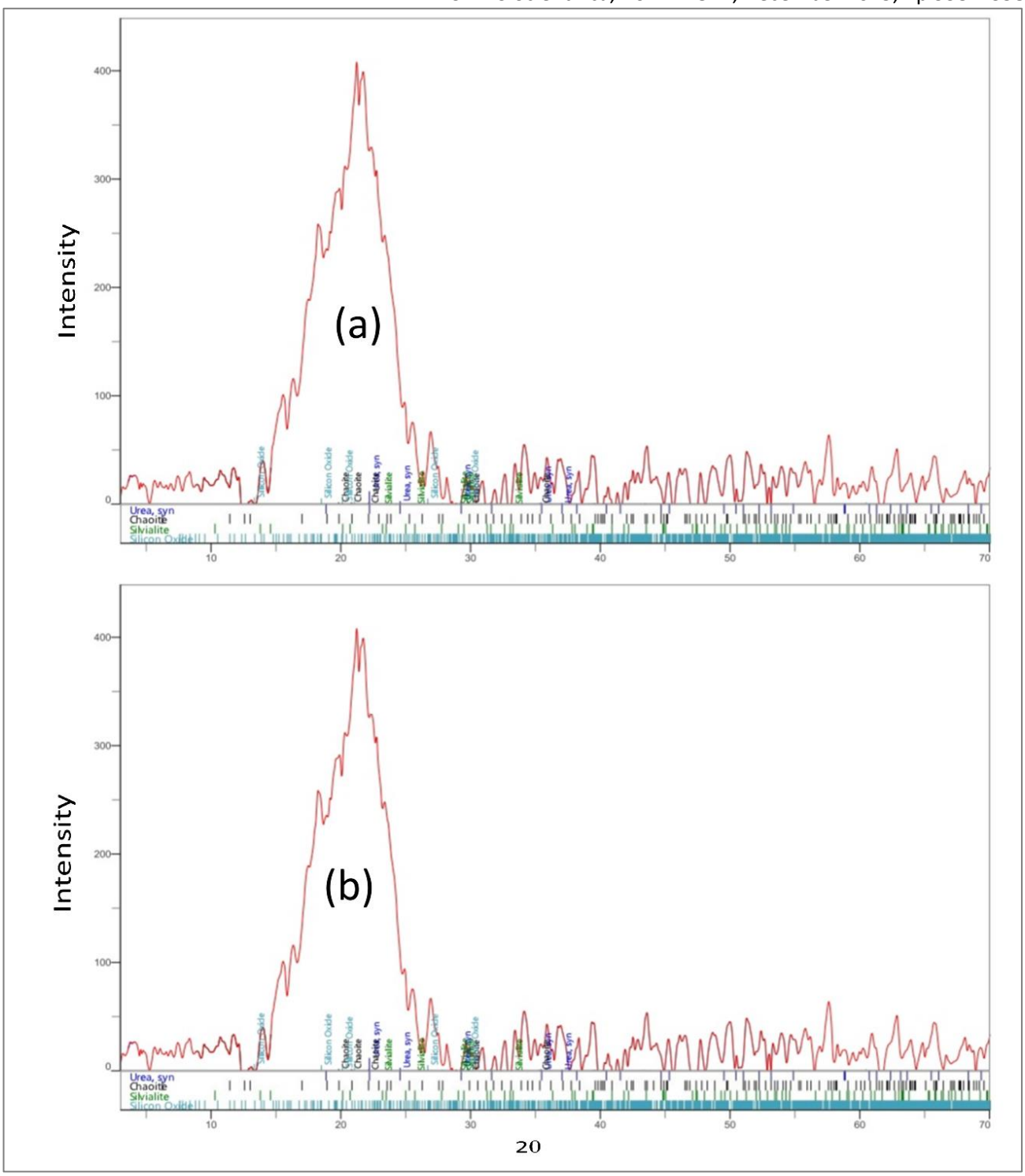

Figure 9: (a) XRD Pattern of Biodegradable polymer composite with fibre (a) and without fibre (b)

The software provided the equation for determining the response (i.e., Tensile strength) using the CCD quadratic model.

Coded Equation

Tensile Strength **(Manikandan and Nagarasampatti Palani, 2025)** = +3.51 +1.66**A** -0.73**B** +0.63**C** -2.97**AB** +2.691**AC** -4.11 **BC** +0.703$\mathbf{A}^2$ +0.25$\mathbf{B}^2$ +1.54$\mathbf{C}^2$ (Kumar *et al.,* 2025)

Where A is the Starch content, B is the Glycerol content, and C is the Fibre content.

The response surface analysis of the tensile strength of starch-based biodegradable plastic films demonstrates the interactive effects of starch, glycerol, and fiber content on the material's mechanical performance. As shown in Figure 4a, tensile strength increased with increasing starch (32.7–35.5 g) and glycerol (13.6–16 mL) contents, reaching a peak of 22.91 MPa, suggesting that higher concentrations of both components enhance film strength to an optimal level (Busu et al., 2021).

In Figure 4b, the interaction between starch and fibre content revealed a curved response surface, indicating that tensile strength increases with fibre addition and that an

optimal starch concentration exists to maximise strength. Finally, Figure 4c shows that tensile strength increases with increasing fibre content (0–3.3 g) due to fibre reinforcement, but decreases with increasing glycerol content (13–16 mL), consistent with glycerol's plasticising effect, which reduces stiffness. The results confirm that optimising the ratios of starch, glycerol, and fibre is crucial for achieving higher tensile strength in biodegradable plastic films, aligning with findings reported by Busu et al. (2021).

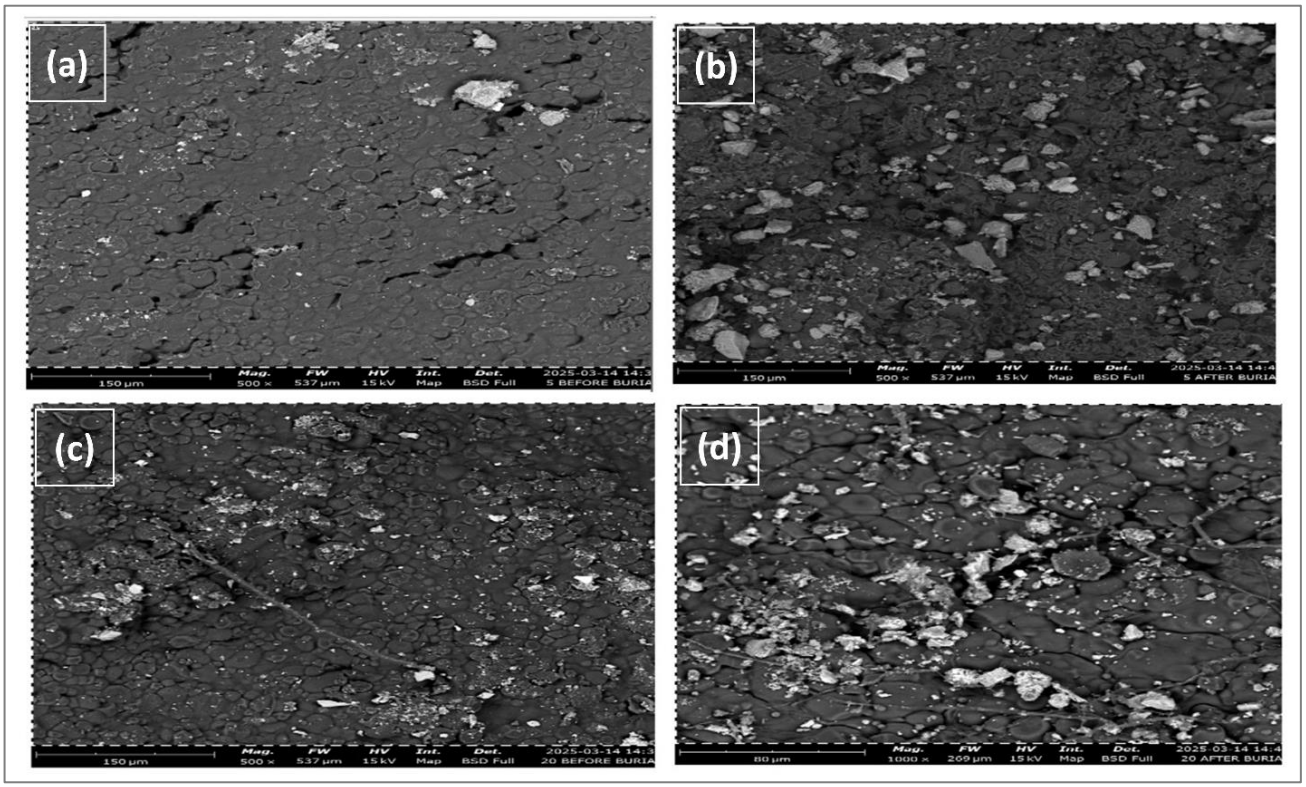

Figure 10: SEM analysis of biodegradable polymer composite before and after burial

The Analysis of Variance (ANOVA) results for the response surface model examining elongation at break reveal significant insights into how various factors and their interactions affect the ductility of the biodegradable polymer composite materials (Table 12). The model's significance is confirmed by a p-value of 0.0012, indicating that at least one factor significantly affects elongation at break. Notably, the interaction terms AB (starch and glycerol) and BC (glycerol and fiber) have highly significant p-values (< 0.0001 and 0.0002, respectively), suggesting that these combinations greatly enhance the material's ductility. In contrast, the main effects of starch and fibre content are not significant, while glycerol content approaches significance (p = 0.0587). The regression equation indicates that increasing glycerol and fibre content tends to decrease elongation, whereas interactions with starch significantly improve it. These findings highlight the critical role of optimizing both individual components and their interactions to achieve desired mechanical properties in biodegradable composite applications.

Analysis of variance result for Elongation at break response surface model

The software provided the equation for determining the response, i.e. Elongation at break, using the CCD quadratic model.

Coded Equation

$$\text{Elongation at break (\%)} = 18.59 + -0.63\mathbf{A} + -2.71\mathbf{B} + (-2.64\mathbf{C}) + 10.43\mathbf{AB} + 3.39\mathbf{AC} + 12.41\mathbf{BC} + (-1.75\mathbf{A}^2) + 5.43\mathbf{B}^2 + 3.15\mathbf{C}^2 \quad (2)$$

Figure 5a shows a 3D surface plot shows a that clearly indicates a correlation between the effect of glycerol content and starch content interaction on elongation at break, the elongation at break represent the flexibility or ductility of the biodegradable composites. as the glycerol content increases elongation at break increases across the entire starch content range, the effect of starch content appears to be less pronounced or more interactive.

Figure 5b shows the 3D plot of the interaction between fibre content and starch content on elongation at break, and it indicates that elongation at break decreases as fibre content increases; the effect of starch content appears to be less dominant or more interactive.

The 3D surface plot of Figure 5c shows a response surface where elongation at break is strongly influenced by both fibre and glycerol content, with a clear interactive effect. As glycerol content increases from 13 to 16ml, elongation at break increases, consistent with the expected effect of the plasticiser. As the fibre content increases, the elongation at break decreases. The result was agreement with the result reported by (Busu *et al.*, 2021).

The ANOVA results for Young's modulus indicate a highly significant model (p-value < 0.0001), confirming that variations in starch, glycerol, and fibre content

significantly influence the material's stiffness (Table 13). The individual contributions of starch content (A) and glycerol content (B) are also significant, with p-values of 0.0025 and 0.0103, respectively, suggesting that both components directly affect the mechanical rigidity of the biodegradable composite. Notably, the interaction terms AB, AC, and BC show extremely significant effects (p-values < 0.0001), indicating that the combinations of these factors lead to substantial changes in Young's modulus. The regression equation shows that increasing starch content enhances stiffness, whereas higher glycerol content negatively affects it, underscoring the complex interplay between these factors. This analysis underscores the importance of optimising the formulation of biodegradable composites to achieve the desired mechanical properties for specific applications, particularly in contexts that demand high stiffness and structural integrity (Draman *et al.*, 2024).

The software provided the equation for determining the response (i.e., young modulus) using the CCD quadratic model.

Coded Equation

Young modulus **(Manikandan and Nagarasampatti Palani, 2025)** = 29.25+ 23.82A + (-18.86B) + 15.49C + -56.54AB + 53.65AC +(-63.85BC) + 14.42A^2 + 9.44B^2 + 16.03C^2 (3)

Figure 6a is a 3D surface plot showing a response surface indicating the the relationship between glycerol content and starch content on young modulus. As glycerol content increases, the young modulus decreases significantly, leading to a much softer material. In the effect of starch content, the plot shows curvature along the starch content axis.

The 3D surface plot of Figure 6b shows the effect of starch content and fibre content interaction on Young's modulus in which the shape of the surface appears relatively flat. As the starch content increases, the young modulus seems to increase, and the effect of the fibre, which also increases the young modulus, appears to slightly increase.

Figure 6c of the 3D surface plot shows the effect of the interaction between the two independent variables (Glycerol and Fibre) on Young's modulus. It shows that as the Young's modulus increases with fibre content, this implies that fibres act as reinforcement in composites, contributing to the structural integrity and load-bearing capacity, thereby increasing the stiffness of the biodegradable composites. The result agreed with that reported by a similar study (Busu *et al.*, 2021).

Thermal properties of the biodegradable polymer composite

The thermal degradation of biodegradable polymer composites at different temperatures and heating rates is shown in Figures 7 and 8, respectively.

Differential Scanning Calorimetry (DSC) analysis revealed key thermal transitions in the biodegradable polymer composites, both with and without kenaf fiber. The glass transition temperature (Tg), observed between 62.5°C and 155°C, showed no significant difference between the two samples, indicating that kenaf fibre incorporation does not significantly affect polymer chain mobility at lower temperatures. The crystallization temperature (Tc) ranged from 170°C to 275°C, with the fiber-free composite exhibiting a sharper and higher Tc (~265°C) compared to the fibre-reinforced composite (~250°C). This reduction suggests that kenaf fibers interfere with molecular packing, thereby hindering crystallization.

The melting temperature (Tm) was observed between 295°C and 325°C, with a sharp peak around 300°C for the composite without fibre, whereas the fibre-reinforced composite showed a lower, broader peak (~340°C) with reduced intensity. This shift indicates a decrease in crystallinity and thermal stability, likely due to the presence of kenaf fibres. Above 350°C, an additional degradation step was observed in the composite without fibre, whereas the kenaf-reinforced sample showed reduced intensity, suggesting that lignocellulosic components in Kenaf accelerate thermal degradation. Overall, the DSC results suggest that kenaf fibre incorporation slightly reduces the crystallinity and thermal stability of starch-based biodegradable composites (Hazrol et al., 2022a, 2023).

Thermogravimetric Analysis (TGA) of the biodegradable polymer composites, with and without kenaf fibre, revealed distinct thermal degradation stages. The first weight loss, occurring between 25 °C and 120 °C, corresponds to moisture evaporation and dehydroxylation, which is more pronounced in fibre-reinforced composites due to Kenaf's hydrophilic nature. The second degradation phase, observed between 200°C and 298°C, is attributed to the breakdown of the polymer matrix and the cellulosic components of the fibers. A third major weight loss between 400°C and 600°C represents the decomposition of organic constituents, including lignin, leaving behind inorganic char residues. The inclusion of kenaf fibers slightly alters the degradation profile, indicating their influence on the composite's thermal stability and resilience (Hazrol et al., 2023).

XRD analysis

The XRD analysis of biodegradable polymer composites was conducted, and the pattern results are shown in Figure 9.

X-ray diffraction (XRD) analysis revealed distinct structural differences between the biodegradable composites with and without kenaf fiber reinforcement. The fibre-reinforced composite exhibited sharp, prominent peaks around 22°, indicating a higher degree of crystallinity, attributed to the cellulose structure of the kenaf fibres. Additional peaks associated with silicate and quartz suggest the presence of inorganic fillers contributing to material stability. In contrast, the composite without fibre showed less intense peaks, indicating lower crystallinity and a more disordered structure. These findings demonstrate that kenaf fiber reinforcement enhances the crystallinity, structural

integrity, and mechanical potential of biodegradable composites (Hazrol et al., 2022a).

Scanning electron microscopy

Results from SEM analysis of biodegradable polymer composite before and after burial are presented in Figure 10a, b, c and d, respectively.

Scanning Electron Microscopy (Oliver-Cuenca *et al.*, 2024) analysis revealed distinct morphological differences between biodegradable composites with and without kenaf fiber, both before and after soil burial. The fibre-free composite initially exhibited a smooth, homogeneous surface with minor voids, suggesting limited reinforcement and potential reduced mechanical strength. After burial, the surface became rougher with increased voids and fragmentation, suggesting extensive microbial degradation. In contrast, the fibre-reinforced composite exhibited a more complex, textured morphology before burial, with visible fibres that enhanced structural integrity through mechanical interlocking. Post-burial images revealed significant surface degradation, fiber fragmentation, and increased porosity, indicating active biodegradation while maintaining partial structural stability. These observations demonstrate that kenaf fiber reinforcement improves the physical structure and mechanical strength of biodegradable composites while supporting controlled biodegradation under soil conditions (Hazrol et al., 2022a).

CONCLUSION

This study demonstrates that starch-based biodegradable plastics reinforced with kenaf fiber can achieve improved material performance through careful formulation. The optimised composites exhibited tensile strength of 22.91 MPa, elongation at break of 59.42%, Young's modulus of 322.46 MPa, water absorption of 85.20%, and biodegradation weight loss ranging from 18.03% to 91.70%. Structural and thermal analyses (FTIR, SEM, XRD, DSC, TGA) confirmed effective fiber–matrix interactions and enhanced thermal stability. Variations in density, thickness, and degradation rates highlighted the influence of starch, glycerol, and fiber ratios on composite properties. These findings provide a quantitative basis for optimising biodegradable composites and for understanding the role of natural fibre reinforcement, without extending claims to commercial applicability or long-term performance.

REFERENCES

Abdel Hamid, E. M., Mohamed, A. E., Mohamed, A. A., Galal, A. A., Mekhemr, A. A., Saleh, E. S., Hassan, M. I., Ahmed, M. H., & Elgendy, S. K. (2025). Optimization of corn starch/glycerol, acetic acid, and cellulose fibers ratio on biodegradable plastic synthesis by Box-Behnken design (BBD). *Clean Technologies and Environmental Policy*, 1-23. [Crossref]

Abotbina, W., Sapuan, S., Sultan, M., Alkbir, M., & Ilyas, R. (2021). Development and characterization of cornstarch-based bioplastics packaging film using a combination of different plasticizers. *Polymers, 13*(20), Article 3487. [Crossref]

Afify, A. H. (2025). Characterizations and Identification of Promoting Plant Growth and Bioagents Bacterial Strains as Indicators for its Productions. *Journal of Agricultural Chemistry and Biotechnology, 16*(7), 105-108. [Crossref]

Agarwal, S., Singhal, S., Godiya, C. B., & Kumar, S. (2023). Prospects and applications of starch based biopolymers. *International Journal of Environmental Analytical Chemistry, 103*(18), 6907-6926. [Crossref]

Ahmad, Z., Razak, N. H. A., Roslan, N. S. M., & Mosman, N. (2014). Evaluation of kenaf fibres reinforced starch based biocomposite film through water absorption and biodegradation properties. *Journal of Engineering Science, 10*, 31.

Akil, H. M., Omar, M. F., Mazuki, A. M., Safiee, S., Ishak, Z. M., & Bakar, A. A. (2011). Kenaf fiber reinforced composites: A review. *Materials & Design, 32*(8-9), 4107-4121. [Crossref]

AlMaadeed, M. A. A., Ponnamma, D., & El-Samak, A. A. (2020). Polymers to improve the world and lifestyle: physical, mechanical, and chemical needs. In *Polymer science and innovative applications* (pp. 1-19). Elsevier. [Crossref]

Azmin, S., Nasrudin, I., Nor, M., Abdullah, P., & Ch'Ng, H. (2024). Development of food packaging bioplastic from potato peel starch incorporated with rice husk silica using response surface methodology comprehending central composite design. *Food Research*.

Badamasi, A., & Salisu, B. (2025). Characterization of Heavy Metal-Tolerant Bacteria from Dumpsites in Katsina Metropolis and their Bioremediation Potential. *Umyu Scientifica, 4*(2), 417-428. [Crossref]

Bergey, D. H. (1994). *Bergey's manual of determinative bacteriology*. Lippincott Williams & Wilkins.

Busu, W. N. W., Chen, R. S., Shahdan, D., Yusof, M. J. M., Saad, M. J., & Ahmad, S. (2021). Statistical optimization using response surface methodology for enhanced tensile strength of polyethylene/graphene nanocomposites. *International Journal of Integrated Engineering, 13*(6), 109-117.

Cerqueira, M. A., Souza, B. W., Teixeira, J. A., & Vicente, A. A. (2012). Effect of glycerol and corn oil on physicochemical properties of polysaccharide films-A comparative study. *Food Hydrocolloids, 27*(1), 175-184. [Crossref]

Çevik, M., & Diambu, A. N. (2024). Advancing Sustainable Development Goals through the Use of Biocomposites for a Greener Future. *Scientific Research Reviews*.

Dan-asabe, B., & Stephen, A. (2018). Mathematical Modelling and Optimization of the Compressive Strength, Hardness and Density of a Periwinkle-Palm Kernel and Phenolic Resin Composite Brake Pad. *Tribology in Industry, 40*(1), 108. [Crossref]

Dan-Asabe, B., Yaro, S., Yawas, D., & Aku, S. (2019). Statistical modeling and optimization of the flexural strength, water absorption and density of a doum palm-Kankara clay filler hybrid composite. *Journal of King Saud University-Engineering Sciences, 31*(4), 385-394. [Crossref]

Dang, X., Guo, B., Du, Y., & Wang, X. (2025). Advancements in Manufacturing and Applications of Starch-Based Antimicrobial Materials. *Polymer Reviews*, 1-40. [Crossref]

Draman, S. F. S., Nursaidin, N., Mohd, N., Daik, R., & El Sheikh, S. (2024). Optimization of Starch-Based Bioplastic from Sweet Potato using Box-Behnken Design with Plasticizer and Filler for Reduced Water Absorption. *Journal of Advanced Research in Fluid Mechanics and Thermal Sciences, 123*(1), 86-94. [Crossref]

Elkaliny, N. E., Alzamel, N. M., Moussa, S. H., Elodamy, N. I., Madkor, E. A., Ibrahim, E. M., Elshobary, M. E., & Ismail, G. A. (2024). Macroalgae bioplastics: a sustainable shift to mitigate the ecological impact of petroleum-based plastics. *Polymers, 16*(9), Article 1246. [Crossref]

Farooq, E., Osama, S. M., Abbas, S. H., & Aqeel, M. (2025). Biodegradable Polymers for Process Intensification in Chemical Engineering: Challenges and Innovations. *Materials Engineering and Innovation, 2*(1), 1-13. [Crossref]

García-Guzmán, L., Cabrera-Barjas, G., Soria-Hernández, C. G., Castaño, J., Guadarrama-Lezama, A. Y., & Rodríguez Llamazares, S. (2022). Progress in starch-based materials for food packaging applications. *Polysaccharides, 3*(1), 136-177. [Crossref]

Gunawardene, O. H., Gunathilake, C., Amaraweera, S. M., Fernando, N. M., Wanninayaka, D. B., Manamperi, A., Kulatunga, A. K., Rajapaksha, S. M., Dassanayake, R. S., & Fernando, C. A. (2021). Compatibilization of starch/synthetic biodegradable polymer blends for packaging applications: A review. *Journal of Composites Science, 5*(11), Article 300. [Crossref]

Hassan, T., Srivastwa, A., Sarkar, S., & Majumdar, G. (2022). Characterization of plastics and polymers: A comprehensive study. *IOP Conference Series: Materials Science and Engineering, 1225*(1), Article 012033. [Crossref]

Hazrol, M., Sapuan, S., Ilyas, R., Zainudin, E., Zuhri, M., & Wahab, N. A. (2022a). Morphology and selected properties of kenaf fiber/cornhusk reinforced corn starch hybrid biocomposites. *Polimery, 67*(11-12), 575-588. [Crossref]

Hazrol, M., Sapuan, S., Zainudin, E., Wahab, N., & Ilyas, R. (2022b). Effect of kenaf fibre as reinforcing fillers in corn starch-based biocomposite film. *Polymers, 14*(8), Article 1590. [Crossref]

Hunter, T. S. (2024). Plastics and petroleum. In *Research Handbook on Plastics Regulation* (pp. 59-78). Edward Elgar Publishing. [Crossref]

Hazrol, M. D., Sapuan, S. M., Ilyas, R. A., Zainudin, E. S., Zuhri, M. Y. M., & Abdul, N. I. (2023). Effect of corn husk fibre loading on thermal and biodegradable properties of kenaf/cornhusk fibre reinforced corn starch-based hybrid composites. *Heliyon, 9*(4). [Crossref]

Ibrahim, F., Salisu, B., Isah, M., & Kaware, M. S. (2024). Isolation and Characterization of Phyllosphere Bacteria and their Bioremediation-Potential of Spent Engine Oil Contaminated Soil. *UMYU Journal of Microbiology Research, 9*(2), 249-260. [Crossref]

Jadhav, H. S., Kate, R. S., Raut, S. A., Kalubarme, R. S., & Kale, B. B. (2023). 8 Carbon and Graphene Nanotubes. *Emerging Applications of Carbon Nanotubes and Graphene*, 106, 161. [Crossref]

Jangong, O., Gareso, P., Mutmainna, I., & Tahir, D. (2019, November). Fabrication and characterization starch/chitosan reinforced polypropylene as biodegradable. In *Journal of Physics: Conference Series* (Vol. 1341, No. 8, Article 082022). [Crossref]

Khoo, P. S., Ilyas, R., Uda, M., Hassan, S. A., Nordin, A., Norfarhana, A., Ab Hamid, N., Rani, M., Abral, H., & Norrrahim, M. (2023). Starch-based polymer materials as advanced adsorbents for sustainable water treatment: current status, challenges, and future perspectives. *Polymers, 15*(14), Article 3114. [Crossref]

Kibet, T., Githinji, D. N., & Nziu, P. (2025). Natural Fibre-Reinforced Starch Biocomposites and Their Effects on the Material Mechanical Properties: A Review. *Advances in Materials Science and Engineering, 2025*(1), Article 9905014. [Crossref]

Koltzenburg, S., Maskos, M., & Nuyken, O. (2017). *Polymer chemistry* (K. Hughes, Trans.). Springer. [Crossref]

Kumar, A., & Bedi, R. (2025). Mechanical and durability properties of sustainable composites derived from recycled polyethylene terephthalate and enhanced with natural fibers: a comprehensive review. *Materials Physics and Mechanics, 53*(1), 117-142.

Kumar, M., Karki, B., & Gope, P. (2025). Kenaf Fiber-Reinforced Biocomposites: A Review of Mechanical Performance, Treatments, and Challenges. *Journal of Materials Engineering and Performance, 16*, 1108.

Manikandan, G., & Nagarasampatti Palani, K. (2025). Adsorption of methylene blue using Ixora coccinea leaf: unveiling the extraordinary potential for sustainable wastewater treatment. *International Journal of Materials Research*. Advance online publication. [Crossref]

Maraveas, C. (2020). Production of sustainable and biodegradable polymers from agricultural waste. *Polymers, 12*(5), Article 1127. [Crossref]

Momeni, S., Craplewe, K., Safder, M., Luz, S., Sauvageau, D., & Elias, A. (2023). Accelerating the biodegradation of poly (lactic acid) through the inclusion of plant fibers: a review of recent advances. *ACS Sustainable Chemistry & Engineering, 11*(42), 15146-15170. [Crossref]

Motaung, T. E., & Linganiso, L. Z. (2018). Critical review on agrowaste cellulose applications for biopolymers. *International Journal of Plastics Technology, 22*(2), 185-216. [Crossref]

Nwuzor, I. C., Oyeoka, H. C., Nwanonenyi, S. C., & Ihekweme, G. O. (2023). Biodegradation of low-density polyethylene film/plasticized cassava starch blends with central composite design for optimal environmental pollution control. *Journal of Hazardous Materials Advances, 9*, Article 100251. [Crossref]

Oliver-Cuenca, V., Salaris, V., Muñoz-Gimena, P. F., Agüero, Á., Peltzer, M. A., Montero, V. A., Arrieta, M. P., Sempere-Torregrosa, J., Pavon, C., & Samper, M. D. (2024). Bio-based and biodegradable polymeric materials for a circular economy. *Polymers, 16*(21), Article 3015. [Crossref]

Park, D.-I., Dong, Y., Wang, S., Lee, S.-J., & Choi, H. J. (2023). Rheological characteristics of starch-based biodegradable blends. *Polymers, 15*(8), Article 1953. [Crossref]

Rajendran, S., Al-Samydai, A., Palani, G., Trilaksana, H., Sathish, T., Giri, J., Saravanan, R., Lalvani, J. I. J., & Nasri, F. (2025). Replacement of Petroleum Based Products With Plant-Based Materials, Green and Sustainable Energy-A Review. *Energy Research, 7*(4), Article e70108. [Crossref]

Saha, A., Kumar, S., & Kumar, A. (2021). Influence of pineapple leaf particulate on mechanical, thermal and biodegradation characteristics of pineapple leaf fiber reinforced polymer composite. *Journal of Polymer Research, 28*(2), Article 66. [Crossref]

Salisu, B., & Ibrahim, F. (2024). Microbial Bioremediation of Spent Engine Oil: Current Advances, Challenges, and Future Directions. *Umyu Scientifica, 3*(4), 260-274. [Crossref]

Salisu, B., Ibrahim, F., Kaware, M. S., & Isah, M. (2025). Gas Chromatographic evaluation of hydrocarbon degradation capabilities of Phyllosphere-derived Bacteria in simulated bioremediation of contaminated soil. *UMYU Journal of Microbiology Research, 10*(1), 21-31. [Crossref]

Sanyang, M. L., Sapuan, S. M., Jawaid, M., Ishak, M. R., & Sahari, J. (2015). Effect of plasticizer type and concentration on tensile, thermal and barrier properties of biodegradable films based on sugar palm (Arenga pinnata) starch. *Polymers, 7*(6), 1106-1124. [Crossref]

Shaikh, M., Haider, S., Ali, T. M., & Hasnain, A. (2019). Physical, thermal, mechanical and barrier properties of pearl millet starch films as affected by levels of acetylation and hydroxypropylation. *International Journal of Biological Macromolecules, 124*, 209-219. [Crossref]

Shen, M., Song, B., Zeng, G., Zhang, Y., Huang, W., Wen, X., & Tang, W. (2020). Are biodegradable plastics a promising solution to solve the global plastic pollution? *Environmental Pollution, 263*, Article 114469. [Crossref]

Spiridon, I., Anghel, N., & Bele, A. (2015). Behavior of biodegradable composites based on starch reinforced with modified cellulosic fibers. *Polymers for Advanced Technologies, 26*(9), 1189-1197. [Crossref]

Thyavihalli Girijappa, Y. G., Mavinkere Rangappa, S., Parameswaranpillai, J., & Siengchin, S. (2019). Natural fibers as sustainable and renewable resource for development of eco-friendly composites: a comprehensive review. *Frontiers in Materials, 6*, Article 226. [Crossref]